Characterization of the *Mycobacterium tuberculosis H37Rv* alkyl hydroperoxidase AhpC points to the importance of ionic interactions in oligomerization and activity

Radha CHAUHAN and Shekhar C. MANDE[1]
Institute of Microbial Technology, Sector 39-A, Chandigarh 160 036, India

An alkyl hydroperoxidase (AhpC) has been found frequently to be overexpressed in isoniazid-resistant strains of *Mycobacterium tuberculosis*. These strains have an inactivated *katG* gene encoding a catalase peroxidase, which might render mycobacteria susceptible to the toxic peroxide radicals, thus leading to the concomitant overexpression of the AhpC. Although the overexpressed AhpC in isoniazid-resistant strains of *M. tuberculosis* may not directly participate in isoniazid action, AhpC might still assist *M. tuberculosis* in combating oxidative damage in the absence of the catalase. Here we have attempted to characterize the AhpC protein biochemically and report its functional and oligomerization properties. The alkyl hydroperoxidase of *M. tuberculosis* is unique in many ways compared with its well-characterized homologues from enteric bacteria. We show that AhpC is a decameric protein, composed of five identical dimers held together by ionic interactions. Dimerization of individual subunits takes place through an intersubunit disulphide linkage. The ionic interactions play a significant role in enzymic activity of the AhpC protein. The UV absorption spectrum and three-dimensional model of AhpC suggest that interesting conformational changes may take place during oxidation and reduction of the intersubunit disulphide linkage. In the absence of the partner AhpF subunit in *M. tuberculosis*, the mycobacterial AhpC might use small-molecule reagents, such as mycothiol, for completing its enzymic cycle.

Key words: decamer, DTT oxidation, mycothiol, peroxidase, thioredoxin.

INTRODUCTION

Isoniazid has been one of the frontline drugs used in tuberculosis control for more than three decades. Resistance to isoniazid develops primarily due to point mutations in the *katG* locus, encoding the catalase peroxidase enzyme [1]. The loss of *katG* function in isoniazid-resistant strains therefore renders *Mycobacterium tuberculosis* susceptible to the toxic peroxide radicals [2]. Under these conditions, overexpression of another gene, *ahpC*, encoding an alkyl hydroperoxide reductase, has been found frequently to occur [3]. In this article we have attempted to characterize the AhpC enzyme biochemically, and to report its functional properties.

The mycobacterial AhpC is a unique enzyme in many ways compared with its well-characterized homologues in enteric bacteria. For example, the *M. tuberculosis* enzyme possesses three cysteine residues, as compared with two in the *Salmonella typhimurium* and *Escherichia coli* enzymes [4,5]. Very recently it has been shown that all three cysteine residues are important for *M. tuberculosis* AhpC activity [6]. Another important difference between the *M. tuberculosis* AhpC and that derived from other closely related species is that the electron-donor partner of AhpC, the FAD/NADPH-binding subunit AhpF, is absent in *M. tuberculosis*, unlike in *E. coli* and *S. typhimurium*. We show here that the mycobacterial AhpC can use dithiothreitol (DTT) as an electron-transfer partner *in vitro*, and rapidly oxidize DTT in the presence of the substrate. Furthermore, we show that unlike its dimeric homologues from enteric bacteria, the mycobacterial AhpC is decameric in nature.

EXPERIMENTAL

M. tuberculosis cloning and purification

The 588 bp-long gene encoding *M. tuberculosis* AhpC was PCR-amplified using the genomic DNA of *M. tuberculosis H37Rv* and overexpressed in the pET23A(+)/*E. coli* BL21 (DE3) expression system. The overexpressed six-histidine-tagged protein, named AhpCHis6, was purified by Ni^{2+}-nitrilotriacetate affinity chromatography. Briefly, cells harbouring pET23A along with the AhpCHis6 insert were grown until they reached a D_{600} of 0.6, and then induced with 0.6 mM isopropyl β-D-thiogalactoside. The lysed cells were centrifuged at 30000 ***g*** for 45 min and the supernatant was loaded on to the Ni^{2+}-nitrilotriacetate column. The column was washed with 50 mM Tris/HCl buffer, pH 7.5, containing 200 mM NaCl and 6% glycerol. The protein was eluted with the same buffer supplemented with 200 mM imidazole. The purity of the protein was checked on SDS/PAGE where it appeared as a single band (results not shown).

Size-exclusion chromatography

Size-exclusion chromatography was performed at room temperature using either the FPLC or SMART systems (Amersham Pharmacia Biotech) equipped with Superdex-200 HR 10/30 or Superdex-200 PC 3.2/30 columns respectively. Calibration of the columns was performed using molecular-mass standards for gel-filtration chromatography supplied by Sigma. Briefly, for calibration of both the columns, thyroglobulin (669 kDa), apoferritin (443 kDa), β amylase (200 kDa), alcohol dehydrogenase

Abbreviations used: DTT, dithiothreitol; TCA, trichloroacetic acid; DTNB, 5,5′-dithiobis-(2-nitrobenzoic acid); Prx, peroxiredoxin; HBP23, 23 kDa haem-binding protein.

[1] To whom correspondence should be addressed (e-mail shekhar@imtech.ernet.in).

(150 kDa), albumin (66 kDa) and carbonic anhydrase (29 kDa) were used as standard markers at the recommended concentrations. Standard proteins were dissolved into equilibration buffer, i.e. 50 mM Tris/HCl buffer, pH 7.5, containing the desired concentration of NaCl. The column was equilibrated and then each protein was applied to the column to determine elution volume (V_e) of the protein. The void volume (V_o) of the column was determined by running Blue Dextran on the column. The calibration curve was plotted as V_e/V_o versus logarithmic molecular mass. No differences in the elution volumes or the calibration curves of the standard proteins were observed when column calibration was performed at different concentrations of NaCl, i.e. 150 mM, 300 mM, 1.5 M or without NaCl.

The columns were equilibrated with at least three bed volumes of the elution buffer prior to each run. Typical flow rates of 0.5 ml/min and 100 μl/min were maintained for the FPLC and SMART systems respectively. Absorbance at 280 nm was measured to monitor elution of the protein from the column. A 3 mg/ml concentration of AhpCHis6 in Tris/HCl, pH 7.5, was used for all the gel-filtration experiments. To study the effect of NaCl concentration on oligomerization, the protein was incubated at various concentrations of NaCl, and the column was equilibrated with the desired concentration of NaCl before loading the protein on each column.

Cross-linking of AhpCHis6

Chemical cross-linking of AhpCHis6 was carried out according to well-established protocols [7,8]. AhpCHis6 (0.5 mg/ml) in triethanolamine buffer, pH 9.0, was incubated with dimethyl pimelimidate for 10 min at 25 °C. To terminate cross-linking, the protein was precipitated with 20 % trichloroacetic acid (TCA). The precipitate was then redissolved in SDS and loaded on to SDS/polyacrylamide electrophoresis gels (10 %).

DTNB [5,5′-dithiobis-(2-nitrobenzoic acid)] assay

Free -SH groups in AhpCHis6 were determined spectrophotometrically at 412 nm using DTNB [9]. AhpC (1.2 μM) was incubated at 25 °C with 0.8 mM DTNB in 50 mM potassium phosphate buffer, pH 7.5. The stoichiometry of the reaction was calculated by using the extinction coefficient of 14150 $M^{-1} \cdot cm^{-1}$ for the thionitrobenzoate (TNB^{2-}) anion in the absence of SDS and a value of 13600 $M^{-1} \cdot cm^{-1}$ in the presence of 5 % SDS. In another experiment, the enzyme was incubated with 5 % SDS for 1 h at room temperature in the presence of 50 mM DTT. Subsequently the excess of DTT was removed by 20 % TCA precipitation. The protein precipitate was washed twice with 20 % TCA and redissolved in 6 M urea/potassium phosphate buffer, pH 7.5. Each assay was repeated three times.

Activity assay by the ferrithiocyanate method

Enzyme activity was monitored by measuring removal of peroxide substrate, t-butyl hydroperoxide, from the reaction mixture. Peroxides form a complex with ferrithiocyanate with an absorption maximum of 480 nm [10,11]. AhpCHis6 protein (44 μM) in potassium phosphate buffer, pH 7.0, containing 1 mM EDTA and 300 mM NaCl, was incubated at 37 °C with 2 mM t-butyl hydroperoxide in a 1 ml reaction mixture. The reaction was initiated by the addition of 10 mM DTT and was terminated by adding 20 % TCA. After the removal of precipitated protein by centrifugation, 0.2 ml of 10 mM ferrous ammonium sulphate and subsequently 0.1 ml of 2.5 M potassium thiocyanate were added to a 1.0 ml aliquot of the supernatant. Absorption of the red ferrithiocyanate complex was measured at 480 nm spectrophotometrically and was compared with t-butyl hydroperoxide standards. K_m and V_{max} values for AhpCHis6 were calculated by following the steady-state kinetics, in which the concentration of substrate, t-butyl hydroperoxide, was varied and the removal of the substrate was measured by the thiocyanate method.

Homology modelling

The sequence homology of *M. tuberculosis* AhpC was investigated by using BLAST to search for similar three-dimensional structures in the Protein Data Bank [12]. Sequence alignment of *M. tuberculosis* AhpC with 1-cysteine and 2-cysteine peroxiredoxins (Prxs) was carried out using CLUSTALW [13]. Coordinates of the 23 kDa haem-binding protein (HBP23; PDB ID 1qq2), from the 2-cysteine Prx family, were used as the template for three-dimensional model constructions. One major insertion of 11 residues in the *M. tuberculosis* AhpC with respect to the HBP23 was modelled as an anti-parallel β-hairpin in continuation with the preceding β-sheet. All other residues that were different between the two proteins were appropriately mutated on a Silicon Graphics workstation using the program O [14]. After performing the mutations, the best side-chain conformations were chosen to avoid short contacts. The resulting model was then energy-minimized using the distance-dependent dielectric constant and other standard parameters in the program DISCOVER.

Fourth-derivative spectra

Absorption spectra and their fourth derivatives were monitored on a Shimadzu UV 1601A spectrophotometer using a derivative interval of 2.0 nm. The enzyme was used at a concentration of 2 mg/ml in 50 mM Tris/HCl buffer, pH 7.5. To reduce the protein, DTT was added to a final concentration of 10 mM. Spectra were recorded over a range of 190–300 nm.

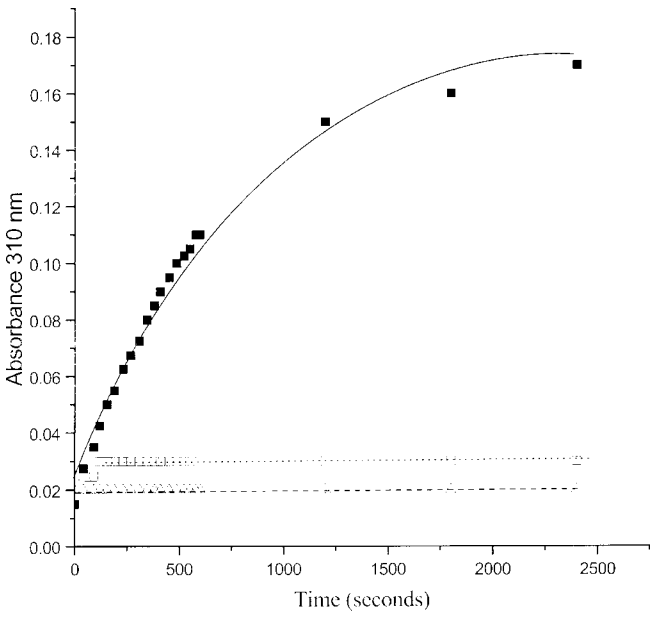

Figure 1 AhpCHis6 catalysed oxidation of DTT

■, The reaction in the presence of AhpCHis6; □, oxidation in the absence of the enzyme; Δ, oxidation in the absence of cumene hydroperoxide. DTT thus can be oxidized only in the presence of the enzyme and the substrate cumene hydroperoxide.

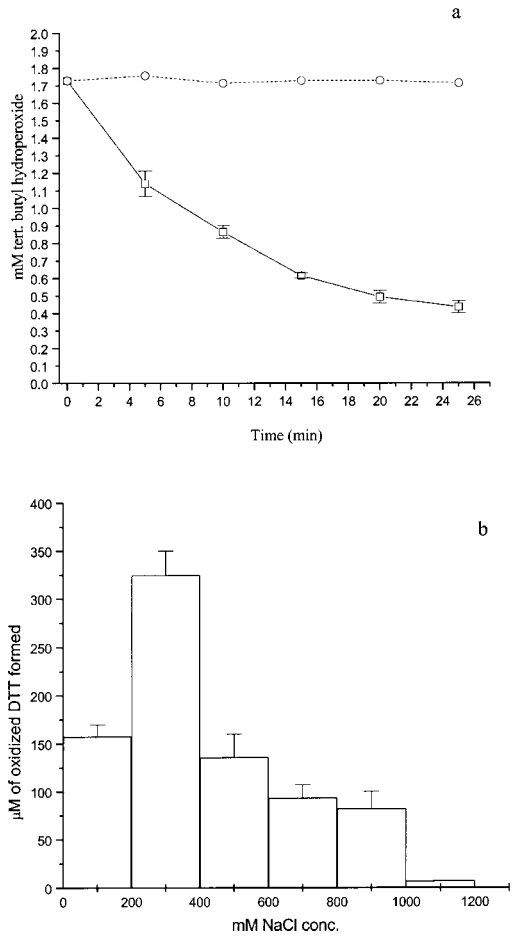

Figure 2 Catalytic activity of AhpCHis6 protein and its dependence on NaCl concentration

(**a**) Removal of peroxides by AhpCHis6 measured by the thiocyanate method. □, The progress of the reaction with enzyme present. ○, Control reactions. (**b**) Enzyme activity of AhpCHis6 measured by the oxidation of DTT as a function of NaCl concentration. The enzyme is most active in the presence of 300 mM NaCl and above this concentration loses its activity rapidly.

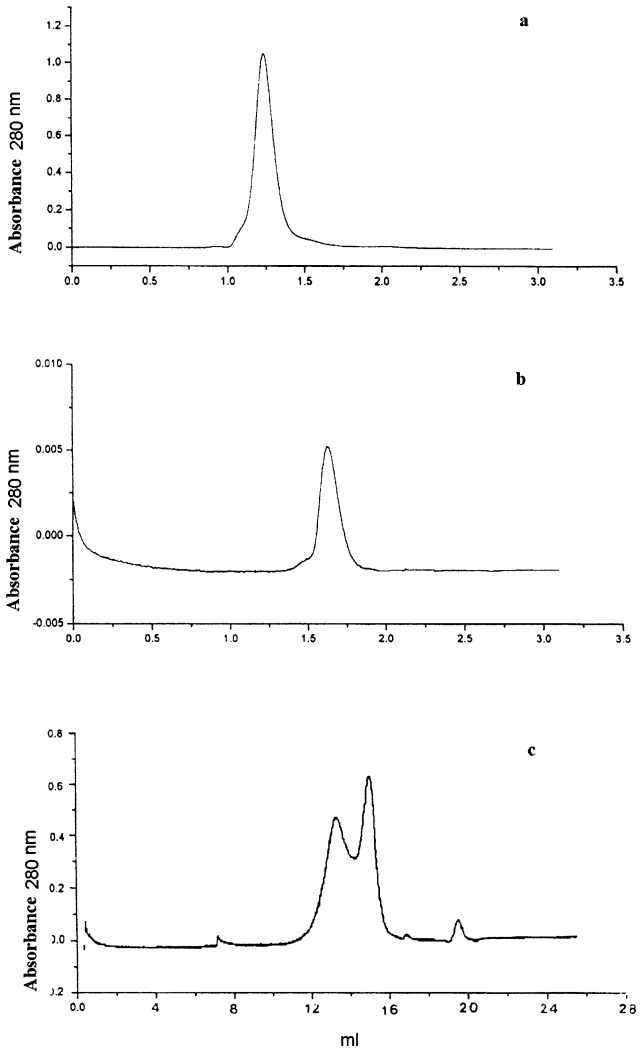

Figure 3 Gel-filtration chromatograms of AhpCHis6

(**a**) The elution profile of the purified AhpCHis6 on a Superdex-200 PC 3.2/30 or Superdex-200 HR 10/30 column. The columns were pre-equilibrated in 50 mM Tris/HCl buffer, pH 7.5, containing 250 mM NaCl before loading the protein. Comparison with standard molecular-mass markers showed that the elution volume corresponded to a 10–12-mer species. (**b**) The elution profile of AhpCHis6 in 1.5 M NaCl. Experimental conditions are as in (**a**), except for the higher salt concentration. The protein clearly eluted as a homogenous dimer in this experiment. (**c**) The elution profile of AhpCHis6 in 1.5 M NaCl and 10 mM DTT. With the addition of DTT, the monomeric species of the enzyme starts to become prominent, in addition to the dimer.

RESULTS

Activity of purified AhpCHis6

The physiological electron donor of mycobacterial AhpC is unknown at present. We chose DTT to perform an activity assay of the recombinant AhpCHis6, since DTT is capable of transferring electrons to peroxides during catalysis in mammalian thiol peroxidases [15]. We found that DTT was oxidized rapidly when both the enzyme and the substrate were present in the reaction mixture. On the other hand, DTT could not be oxidized when either the enzyme or the substrate, or both, were omitted from the reaction mixture. Similarly, when AhpC was replaced with BSA for monitoring the desired activity, DTT was not oxidized (Figure 1).

To confirm the enzymic activity, a thiocyanate assay [11] was performed to measure a decrease in substrate concentration, as described in the Experimental procedures section. Upon incubation of the enzyme with t-butyl hydroperoxide and DTT, a continuous decrease in the amount of t-butyl hydroperoxide was observed as the reaction proceeded. In contrast, control reactions without the enzyme, or with BSA in place of AhpCHis6, showed a constant absorbance at 480 nm (Figure 2a). These results therefore indicated that the recombinant AhpCHis6 was fully functional and was capable of catalysing the reduction of t-butyl hydroperoxide using DTT as an electron-transfer partner.

On probing the effect of NaCl on the enzyme activity, we found that enzyme activity increased gradually with NaCl concentration and that it was optimal at 300 mM NaCl. On increasing the concentration of NaCl further, there was a significant decrease in the DTT oxidation (Figure 2b). The loss of activity at higher concentrations of NaCl, particularly at 1.5 M, is indicative of the important role of ionic interactions during catalysis. Inspection of the three-dimensional model showed the presence of a chloride-ion-binding site next to the active-site cysteine residues. This region, although partially solvent-shielded, is dominated by the presence of charged side-

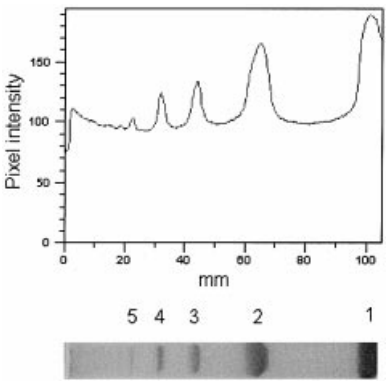

Figure 4 SDS/PAGE (10%) scans showing cross-linked subunits of AhpCHis6

Molecular masses of the bands are as follows: band 1, 25 kDa; band 2, 43 kDa; band 3, 68 kDa; band 4, 98 kDa; band 5, 120 kDa. These molecular masses correspond, respectively, to the monomer and cross-linked dimer, trimer, tetramer and pentamer of AhpCHis6. Beyond the pentamer, other species are notably absent, suggesting that the basic unit of quaternary structure is a pentamer.

Table 1 DTNB titration of AhpCHis6

Pretreatment	Free thiol groups (RSH)/AphCHis6 monomer (μmol of RSH/μmol of subunit)
Native AhpC	0.76 ± 0.1
AhpC + 5% SDS	0.68 ± 0.01
AhpC + 50 mM DTT + 5% SDS	2.46 ± 0.17

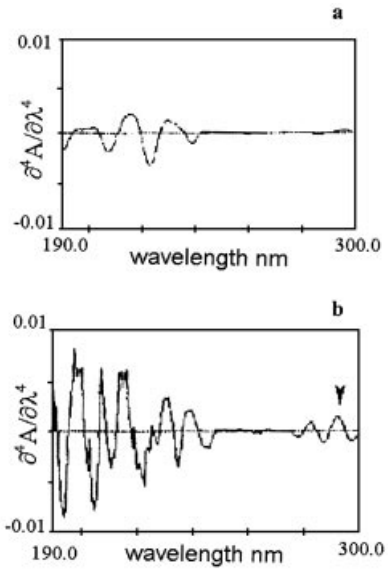

Figure 5 Fourth-derivative absorption spectra of (a) reduced and (b) oxidized AhpCHis6

The change due to tryptophan residues is indicated in (**b**) by an arrowhead, showing clearly a change in the environment of tryptophan residues in the two states. This change presumably takes place in the neighbourhood of Trp-47 and Trp-96, as discussed in the text.

chain residues Glu-64, Arg-133 and Arg-156. We thus believe that activity of the enzyme may be lost at higher salt concentrations due to the screening effect on electrostatic interactions.

To confirm the NaCl-dependent activity of AhpCHis6, we calculated the K_m and V_{max} kinetic parameters in the presence of 100 and 300 mM NaCl. In accordance with the increased activity of the enzyme, we observed that the K_m of AhpCHis6 in 300 mM NaCl was 35 mM, compared with 8 mM in the presence of 100 mM NaCl. However, not only K_m was affected; V_{max} also doubled in 300 mM NaCl (results not shown). Thus, the enhanced activity of the enzyme at 300 mM NaCl ionic strength cannot be explained based solely on the reduced substrate affinity. Nonetheless, the salt concentration-dependence suggests an important role of ionic interactions in catalytic activity of the enzyme.

Oligomeric assembly of recombinant AhpCHis6

In order to determine if the loss of activity at higher NaCl concentrations is attributed to the loss of quaternary structure of the enzyme, we performed size-exclusion chromatography. Results of the experiments in the presence of 250 mM NaCl, quite unexpectedly, showed that the molecule migrated as a mass of 253 kDa on analytical gel-filtration column, unlike its dimeric homologues from other bacteria. The homogeneity of this peak suggested that AhpCHis6 might form a 10–12-mer in solution (Figure 3a). Although we could not perform a similar experiment in absence of NaCl due to the instability of the protein, we believe that the protein would possess the same oligomeric structure in the absence of salt.

The activity of AhpCHis6, as mentioned earlier, was reduced considerably at high concentrations of NaCl. Size-exclusion chromatography showed that, in the presence of 1.5 M NaCl, the decamer disintegrated into a dimer (Figure 3b). The dimer, obtained in 1.5 M NaCl, dissociated further into monomers in the presence of 10 mM DTT (Figure 3c). The dissociation of dimers into monomers in the presence of DTT suggested the presence of an intersubunit disulphide linkage in the protein. These results thus indicated that the oligomeric assembly of AhpCHis6 might be stabilized through ionic interactions. Since the activity of AhpCHis6 is attributed to decameric quaternary structure, it seems that in the cellular environment the protein maintains its decameric assembly.

To further investigate the pattern of AhpCHis6 oligomerization, we cross-linked the AhpCHis6 with the ϵ-amine-specific cross-linker, dimethyl pimelimidate, followed by SDS/PAGE of the cross-linked species. Five major species were observed and the molecular-mass values corresponded to those calculated for the monomer, dimer, trimer, tetramer and pentamer (Figure 4). As such the data indicate that the fundamental unit of quaternary structure is a 'pentamer'. Furthermore, since analytical gel-filtration data show that AhpCHis6 is a 10–12-mer, the likelihood is that AhpCHis6 has a paired pentameric subunit arrangement.

The role of cysteines and ionic interactions in the oligomerization of AhpCHis6

The purified AhpCHis6 appears as a single band of molecular mass 25 kDa on SDS/PAGE when reduced with β-mercaptoethanol. However, under non-reducing conditions several high-molecular-mass bands were also observed. The most prominent

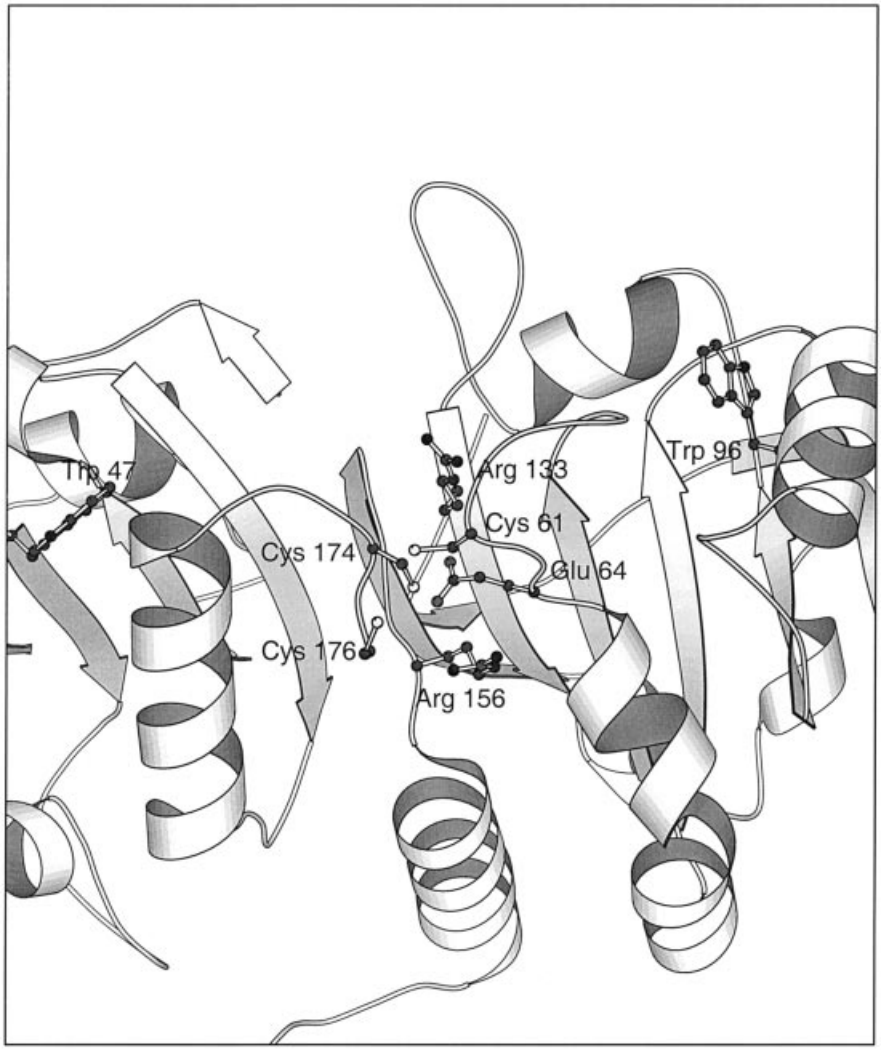

Figure 6 Ribbon diagram of the model constructed using 2-cysteine Prx co-ordinates

The three catalytically important cysteines are shown. The importance of charged residues is highlighted by the presence of Glu-64, Arg-133 and Arg-156 next to the active site. Two tryptophan residues, Trp-47 and Trp-96, which we believe give rise to differences in the absorption spectra, are also shown. The figure was produced using MOLSCRIPT [29].

of these bands corresponded to a molecular mass of ≈ 45 kDa, suggesting the presence of a dimeric species. The absence of a dimer under reducing conditions and its presence under non-reducing conditions suggests an intersubunit disulphide bond. Thus monomers within a dimer are likely to be held together by disulphide linkages.

The amino acid sequence of mycobacterial AhpC contains a total of three Cys residues. To confirm if the cysteines, by some means, were responsible for the multimeric aggregation of the protein, a DTNB assay was carried out. The total numbers of free thiol groups in AhpCHis6 estimated from DTNB analysis under various treatments are listed in Table 1. These results showed clearly that there was only one free thiol group per subunit of purified recombinant AhpCHis6. On the other hand, treatment of AhpCHis6 with 10 mM DTT along with 5% SDS resulted in all the three cysteines in their reduced forms. Thus the protein possessed only one disulphide bond per monomer in its oxidized state. This disulphide bond, as we have shown earlier, cross-linked the two monomers in a dimer. Consequently the third cysteine was not involved in any disulphide linkage, ruling out possible oligomerization arising from disulphide bonds.

Conformational changes in recombinant AhpCHis6

UV absorption fourth-derivative spectra of the oxidized and reduced protein are shown in Figure 5. These spectra showed significant differences between the oxidized and the reduced states of the protein. The fourth-derivative spectra of the oxidized protein revealed a peak at 290 nm, corresponding to tryptophan residues. This peak was absent in AhpCHis6 protein reduced with 10 mM DTT (Figure 5). The derivative spectra therefore indicated that tryptophan residues were exposed to the solvent in the oxidized form of the protein but were solvent-shielded in the reduced AhpCHis6. A conformational change is thus likely to occur during oxidation/reduction of the protein.

The three-dimensional model of the protein generated using HBP23 co-ordinates [16] was inspected to obtain insights into possible conformational changes. The model showed that Cys-61 of one subunit is cross-linked with Cys-174 of another (Figure 6). The model also showed two partially solvent-exposed tryptophan residues, 47 and 96, in the vicinity of the active site. These two tryptophan residues are likely to be affected most by conformational changes related to oxidation/reduction of the protein, due to their proximity to the loops containing all three important cysteine residues. Thus movement of the loops containing Cys-61, Cys-174 and Cys-176 is likely to lead to burial of Trp-47 and Trp-96, which are otherwise solvent-exposed in the oxidized protein.

DISCUSSION

M. tuberculosis lacks the classical oxidative stress responses, with the *oxyR* regulator being absent from its genome [17,18]. In the absence of OxyR-regulated defence, the catalase peroxidase enzyme encoded by the *katG* gene has been found to be the only peroxide-inducible gene in *M. tuberculosis*. The isoniazid-resistant strains of *M. tuberculosis* are therefore especially susceptible to oxidative damage due to the non-functional catalase peroxidase. In the absence of a functional *oxyR* response and the malfunctional *katG*, the tuberculosis bacilli are therefore faced with an unusual situation of survival within the host's macrophages without an effective oxidative stress response. In these strains of *M. tuberculosis*, the *ahpC* gene has been shown to be frequently overexpressed [19]. AhpC has also been shown to be vital for mycobacterial survival within macrophages [20], and is therefore an attractive drug target. We have undertaken work to biochemically characterize this important enzyme.

Eubacteria such as *E. coli*, *S. typhimurium* and *Bacillus subtilis* possess AhpF protein as an electron-donor partner of AhpC [4,21,22]. While in yeast and mammalian systems, the thioredoxin/thioredoxin reductase system substitutes AhpF [15,23]. It has also been shown that NADH oxidase can also reduce AhpC in *Amphibacillus xylanus* [24]. Hence, it appears that there is no common electron-transfer partner of AhpC. All these partners known to date share only one common characteristic, i.e. they are FADH/NAD(P)H-binding proteins. Therefore in the absence of AhpF protein *M. tuberculosis* may use thioredoxin or NADH oxidase as an electron-donating partner during catalysis.

On the basis of our results of DTT oxidation we found that DTT can transfer electrons to substrate via AhpC, which suggests that the mycobacterial AhpC may use a small molecule as an electron-transfer partner. Hence, we hypothesize that the possible electron donor of mycobacterial AhpC could be either thioredoxin or mycothiol, a major low-molecular-mass thiol, analogous to glutathione. Our speculations are also supported by the findings that genes responsible for mycothiol synthesis can be induced by oxidative stress [25]. These speculations need further experimental evidence, and studies are underway in our laboratory.

Interestingly, we found that the activity of the alkyl hydroperoxidase enzyme was dependent on salt concentration. Our findings that the enzyme was most active at 300 mM NaCl are surprising since the physiological salt concentration in the cellular environment is far less than 300 mM. The three-dimensional model of mycobacterial AhpC indicated the presence of a chloride-ion-binding site in AhpC. Earlier it has been reported that human 2-cysteine Prx binds to chloride ions to maintain the active-site structure [16], which confirms our results. The occurrence of several charged side chains in the proximity of the catalytic cysteine residues suggests that these side chains may be crucial for the maintenance of the active-site configuration. All the charged side chains in the active site are conserved in evolution and thus support our observation that ionic interactions may play a crucial role in the activity of mycobacterial AhpC.

To probe whether ionic interactions were important for subunit association, and if the loss of activity was a consequence of disintegration of subunit structure, we carried out gel-filtration experiments. Whereas we were expecting the enzyme to be dimeric in nature, similar to its homologues from other bacteria, the mycobacterial enzyme interestingly showed that it is decameric. Decamerization has previously been reported for AhpC from *A. xylanus* [26] and human TPx-B [27]. There is no report available yet on the physiological state of mycobacterial AhpC oligomerization and its role *in vivo* in oxidative stress.

Very recently the oligomeric nature of mycobacterial AhpC has also been reported by Hillas et al. [6]. Although the previous report on mycobacterial AhpC was not certain about the number of subunits in the oligomer, we have shown conclusively here that the enzyme is a decamer, through a combination of chemical cross-linking studies and precise analytical gel-filtration experiments. Further, the decamer of AhpCHis6 could be dissociated at high salt concentrations, making the dimer a dominant species. The dimers could be dissociated into monomers only under reducing conditions, implying presence of an intersubunit disulphide linkage.

The intersubunit disulphide has been observed in the structure of 2-cysteine Prx, but has been suggested to be formed only during the catalytic cycle [16,28]. The equivalent cysteine residues in *M. tuberculosis* would be Cys-61 and Cys-174 derived from two different subunits. Interestingly, the mycobacterial AhpC contains a cysteine residue at position 176 in the sequence, very close to the intersubunit disulphide, as observed in the three-dimensional model. The third cysteine residue could be modelled successfully in the three-dimensional structure, contrary to the suggestion of Hillas et al. [6]. All three cysteine residues have very recently been shown to be crucial for the activity of the enzyme by site-directed mutagenesis studies [6]. This gives rise to an interesting speculation that Cys-174 and Cys-176 may be involved in a disulphide link, reduction of which leads to the formation of the intersubunit Cys-61–Cys-174 disulphide bond.

In our three-dimensional model of AhpCHis6, we found that Trp-47 and Trp-96 are exposed to solvent in the oxidized state of the enzyme. This observation is consistent with our UV absorption-spectra studies. During oxidation and reduction of AhpCHis6, there is rearrangement of Trp-47 and Trp-96. Such rearrangement arises due to the movement of loops containing Cys-61, Cys-174 and Cys-176, which lead to burial of Trp-47 and Trp-96 in the reduced state of AhpCHis6. Such types of conformational change have also been observed for human TPx-B and other bacterial AhpCs [27,28].

Biochemical characterization of *M. tuberculosis* AhpC thus shows that ionic interactions play an important role in its function as well as oligomerization. These results should lead to the initiation of work on rational drug design using this enzyme as a potential target.

We thank Jaya Tyagi for the supply of *M. tuberculosis H37Rv* genomic DNA, Nandita Bachhawat, Bhupesh Taneja and Pradip Chakraborti for help in cloning and purification of proteins, and Sagar Nimsadkar for technical assistance. We also thank Girish Sahni and Purnananda Guptasarma for access to the chromatographic equipment, and for stimulating discussions. R. C. is a Council of Scientific and Industrial Research (CSIR) junior research fellow. Financial assistance from CSIR and the Department of Biotechnology to S.C.M. is gratefully acknowledged.

REFERENCES

1 Zhang, Y., Heym, B., Allen, B., Young, D. and Cole, S. (1992) The catalase-peroxidase gene and isoniazid resistance of *Mycobacterium tuberculosis*. Nature (London) **358**, 591–593

2 Dhandayuthapani, S., Zhang, Y., Mudd, M. H. and Deretic, V. (1996) Oxidative stress response and its role in senstivity to isoniazid in mycobacteria: characterization and inducibility of *ahpC* by peroxides in *Mycobacterium smegmatis* and lack of expression in *M. aurum* and *M. tuberculosis*. J. Bacteriol. **178**, 3641–3649

3 Sherman, D. R., Mdluli, K., Hickey, M. J., Arain, T. M., Morris, S. L., Barry III, S. E. and Stover, C. K. (1996) Compensatory *ahpC* gene expression in isoniazid resistant *Mycobacterium tuberculosis*. Science **272**, 1641–1643

4 Storz, G., Fredric, S. J., Tartaglia, L. A., Morgan, R. W., Silveria, L. A. and Ames, B. N. (1989) An alkyl hydroperoxide reductase induced by oxidative stress in *Salmonella typhimurium* and *Escherichia coli*: genetic characterization and cloning of *ahp*. J. Bacteriol. **171**, 2049–2055

5 Christman, M. F., Storz, G. and Ames, B. N. (1989) OxyR, a positive regulator of hydrogen peroxide-inducible genes in *Escherichia coli* and *Salmonella typhimurium*, is homologous to family of bacterial regulatory proteins. Proc. Natl. Acad. Sci. U.S.A. **86**, 3484–3488

6 Hillas, P. J., Alba, F. S. D., Oyarzabal, J., Wilks, A. and Montellano, O. D. (2000) The AhpC and AhpD antioxidant defence system of *Mycobacterium tuberculosis*. J. Biol. Chem. **275**, 18801–18809

7 Thomas, J. O. (1989) Chemical crosslinking of histones. Methods Enzymol. **170**, 549–571

8 Tae, H. J. (1983) Bifunctional reagents. Methods Enzymol. **91**, 580–606

9 Riddles, P. W., Blakeley, R. L. and Zerner, B. (1979) Elleman's reagent: 5,5′ dithiobis (2-nitro benzoic acid) — a reexamination. Anal. Biochem. **94**, 75–81

10 Cha, M. K. and Kim II, H. (1996) Glutathione linked thiol peroxidation activity of human serum albumin: a possible antioxidant of serum albumin in blood plasma. Biochem. Biophys. Res. Commun. **222**, 619–625

11 Thurman, R. G., Ley, H. G. and Scholz, R. (1972) Hepatic microsomal ethanol oxidation: hydrogen peroxide formation and the role of catalase. Eur. J. Biochem. **25**, 420–430

12 Altschul, S. F., Miller, W., Myers, E. W. and Lipman, D. J. (1990) Basic local alignment search tool. J. Mol. Biol. **215**, 403–410

13 Higgins, D. G. and Sharp, P. M. (1988) CLUSTAL: a package for performing multiple alignments on microcomputer. Gene **73**, 237–244

14 Jones, T. A., Zou, J. Y., Cowan, S. W. and Kjeldgaard, M. (1991) Improved method for building protein models in electron density maps and the location of errors in these models. Acta Crystallogr. **A47**, 110–119

15 Kang, S. W., Baines, I. C. and Rhee, S. G. (1998) Characterization of a mammalian peroxiredoxin that contains one conserved cysteine. J. Biol. Chem. **273**, 6303–6311

16 Hirotsu, S., Abe, Y., Kengo, O., Nagahara, N., Hori, H., Nishino, T. and Hakoshima, T. (1999) Crystal structure of multifunctional 2-Cys peroxiredoxin heme binding protein 23 kDa/proliferation associated gene product. Proc. Natl. Acad. Sci. U.S.A. **96**, 12333–12338

17 Deretic, V., Phillip, W., Dhandayuthapani, S., Mudd, M. H., Curcic, R., Garbe, T., Heym, B., Via, T. E. and Cole, S. T. (1995) *Mycobacterium tuberculosis* is a natural mutant with an inactivated oxidative stress regulatory gene: implications for sensitivity to isoniazid. Mol. Microbiol. **17**, 889–900

18 Cole, S. T., Brosch, R., Parkhill, J., Garnier, T., Churcher, C., Harris, D., Gordon, S. V., Eiglmeier, K., Gas, S., Barry III, C. E. et al. (1998) Deciphering the biology of *Mycobacterium tuberculosis* from the complete genome sequence. Nature (London) **393**, 537–544

19 Wilson, T. M. and Collins, D. M. (1996) *ahpC*, a gene involved in isoniazid resistance of the *Mycobacterium tuberculosis* complex. Mol. Microbiol. **19**, 1025–1034

20 Wilson, T., Lisle de, G. W., Marcinkeviciene, J. A., Blanchard, J. S. and Collins, D. M. (1998) Antisense RNA to *ahpC*, an oxidative stress defence gene involved in isoniazid resistance, indicates that AhpC of *Mycobacterium bovis* has virulence properties. Mol. Microbiol. **144**, 2687–2695

21 Jacobson, F. C. S., Morgan, R. W., Christman, M. F. and Ames, B. N. (1989) An alkyl hydroperoxide reductase from *Salmonella typhimurium* involved in the defence of DNA against oxidative damage. J. Biol. Chem. **264**, 1488–1496

22 Antelmann, H., Engelmann, S., Schimid, R. and Hecker, M. (1996) General and oxidative stress in *Bacillus subtilis*: cloning, expression and mutation of the alkyl hydroperoxide reductase operon. J. Bacteriol. **178**, 6571–6578

23 Chae, H. Z., Chung, S. J. and Rhee, S. G. (1994) Thioredoxin dependent peroxide reductase from yeast. J. Biol. Chem. **269**, 27670–27678

24 Nimura, Y. and Massey, V. (1996) Reaction mechanism of *Amphibacillus xylanus* NADH oxidase/alkyl hydroperoxide reductase flavoprotein. J. Biol. Chem. **271**, 30459–30464

25 Bornnemann, C., Jardine, M. A., Spies, H. S. C. and Steencamp, D. J. (1997) Biosynthesis of mycothiol: elucidation of the sequence of steps in *Mycobacterium smegmatis*. Biochem. J. **325**, 623–629

26 Kitano, K., Nimura, Y., Nishiyama, Y. and Miki, K. (1999) Stimulation of peroxidase activity by decamerization related to ionic strength: AhpC protein from *Amphibacillus xylanus*. J. Biochem. (Tokyo) **126**, 313–319

27 Schroder, E., Littlechild, J. A., Lebedev, A. A., Errington, N., Vagin, A. A. and Isupov, M. N. (2000) Crystal structure of decameric 2-cysteine peroxiredoxin from human erythrocytes at 1.7 Å resolution. Structure **8**, 605–615

28 Ellis, H. R. and Poole, L. B. (1997) Requirement for the two AhpF cysteine disulfide centres in catalysis of peroxide reduction by alkyl hydroperoxide reductase. Biochemistry **36**, 13349–13356

29 Kraulis, P. J. (1991) MOLSCRIPT: a program to produce both detailed and schematic plots of protein structures. J. Appl. Crystallogr. **24**, 946–950

Received 14 September 2000/7 November 2000; accepted 1 December 2000